Supplemental Figure 1

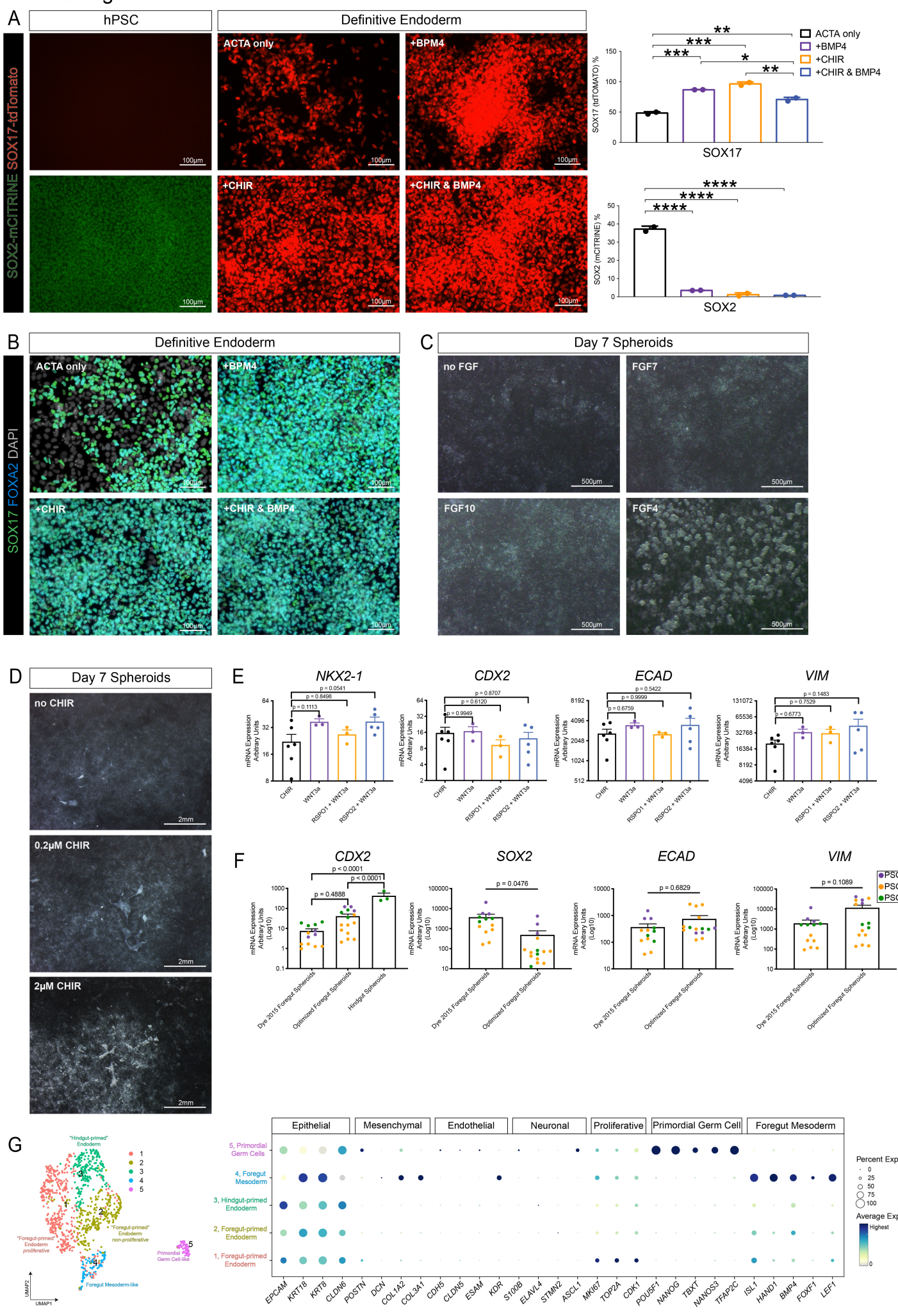

Fig. S1. Optimization of Directed Differentiation of hPSCs at Definitive Endoderm, Foregut Spheroid and NKX2-1$^+$ Spheroid Stages, Related to Figure 1

(A) (Left) SOX2-mCitrine (pluripotent stem cell marker) and SOX17-tdTomato (definitive endoderm marker) reporter images of SOX2-mCITRINE and SOX17-tdTomato on hPSCs and hPSC-derived day 4 definitive endoderm (DE) where 50ng/mL BMP4 and/or 2μM CHIR were added on day 1 of a 3-day 100ng/mL Activin A (ACTA) treatment to induce DE (see Fig. 1A) in a hPSC line expressing SOX2-mCitrine/SOX17-tdTomato hPSC line (Martyn *et al.*, 2018). (Right) Flow cytometry quantifications of day 4 DE cultures. Two technical replicates from the same experiment were performed for flow cytometry quantifications. Statistical tests were performed by ordinary one-way ANOVA.

(B) Immunofluorescence staining for the DE markers SOX17 and FOXA2 on day 4 DE testing conditions as noted in S1A. This experiment was performed on two independent hPSC lines different than the reporter line in Fig. S1A. Representative images are shown from H9 ESCs.

(C) Brightfield images of day 7 spheroids evaluated for FGF-dependent spheroid formation. Conditions include no FGF, 10ng/mL FGF7, 500ng/mL FGF10, or 500ng/mL FGF4 on days 4 – 6.

(D) Brightfield images of day 7 spheroids evaluated for WNT-dependent spheroid formation. Conditions include no CHIR99021, 0.2μM CHIR99021, or 2μM CHIR99021 on days 4 – 6.

(E) RT-qPCR data comparing expression of the lung epithelial marker *NKX2-1*, the hindgut epithelial marker *CDX2*, the pan-epithelial marker *ECAD*, and the pan-mesenchymal marker *VIM* when CHIR99021, WNT3a, RSPO1 & WNT3a, or RSPO2 & WNT3a was used to activate WNT signaling on days 7 – 9 of the NKX2-1-optimized spheroid directed differentiation protocol. Data points for CHIR99021 and WNT3a + RSPO2 represent 2 independent experiments with 2 – 3 technical replicates and data points from other conditions represent one independent experiment with 3 technical replicates. All experiments were performed on H9 ESCs. Statistical tests compared all conditions to CHIR99021 and were performed by ordinary one-way ANOVA followed by Dunnett's multiple comparison test.

(F) RT-qPCR data comparing expression of the hindgut epithelial marker *CDX2*, the posterior foregut marker *SOX2*, the pan-epithelial marker *ECAD*, and pan-mesenchymal marker *VIM* from previously published foregut spheroids (Dye *et al.*, 2015) to optimized foregut spheroids, and in the case of *CDX2*, hindgut spheroids. Each color represents an independent experiment with a unique iPSC line (purple: WTC11, orange: iPSC17 WT 7B2, green: iPSC line 72.3). Each data point of the same color represents a technical replicate from the same iPSC line in one or more independent experiments. Error bars represent standard error of the mean. Statistical test for *CDX2* was performed by ordinary one-way ANOVA followed by Tukey's multiple comparison test and statistical tests for the remaining markers was performed by unpaired Welch's one-tailed t-tests.

(G) Cluster plot of scRNA-seq data from day 10 spheroids and dot plot of epithelial, mesenchymal, endothelial, and neuronal lineage genes as well as proliferation markers in each cluster of the UMAP. The dot size represents the percentage of cells expressing the gene in the corresponding cluster, and the dot color indicates log-normalized expression level of the gene.

Supplemental Figure 2

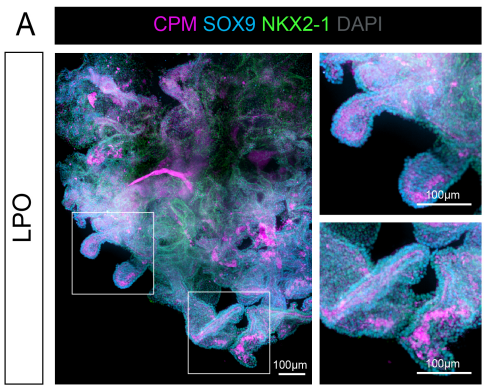

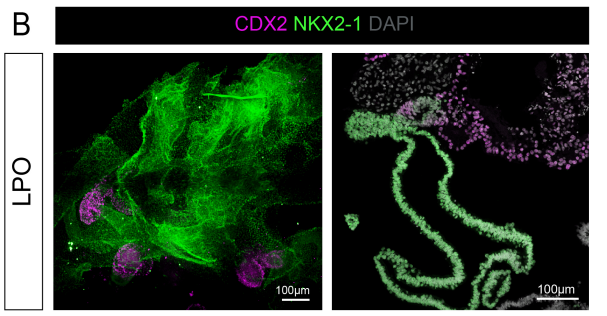

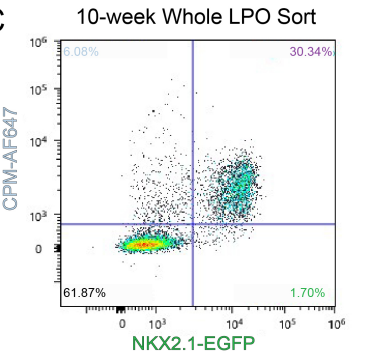

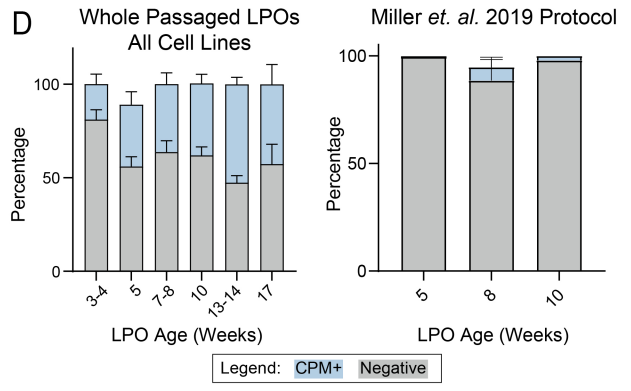

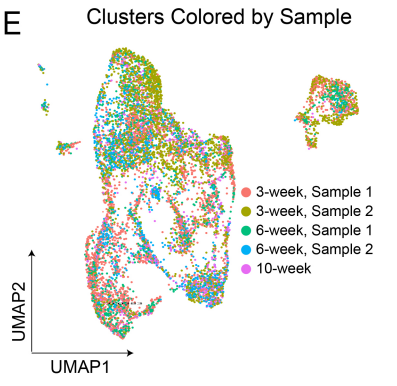

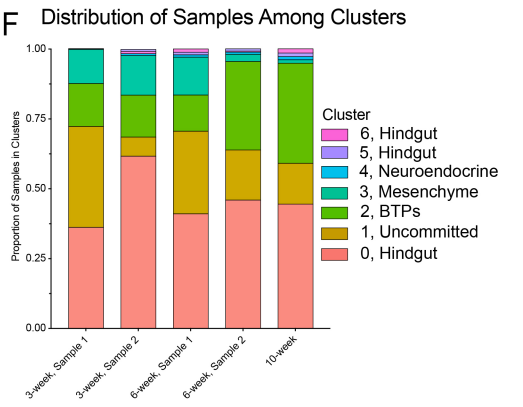

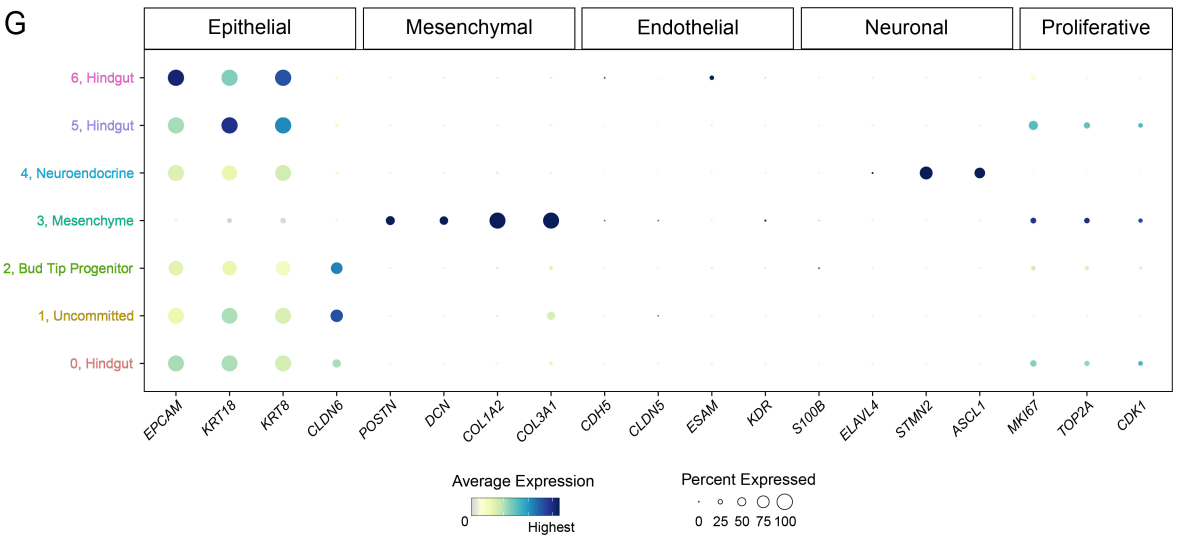

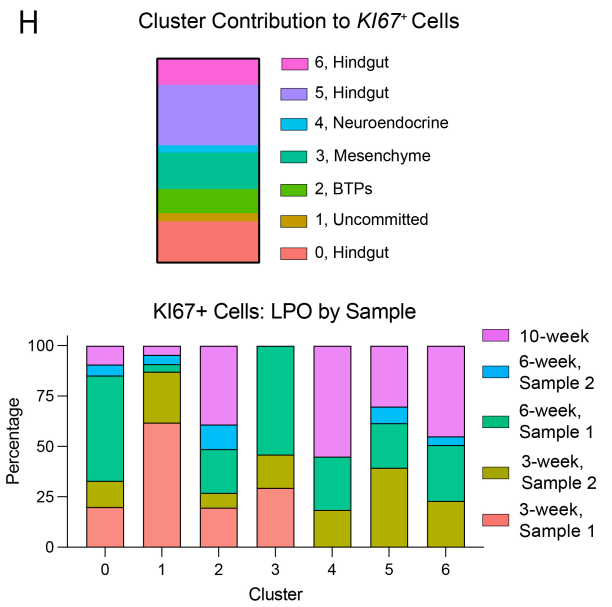

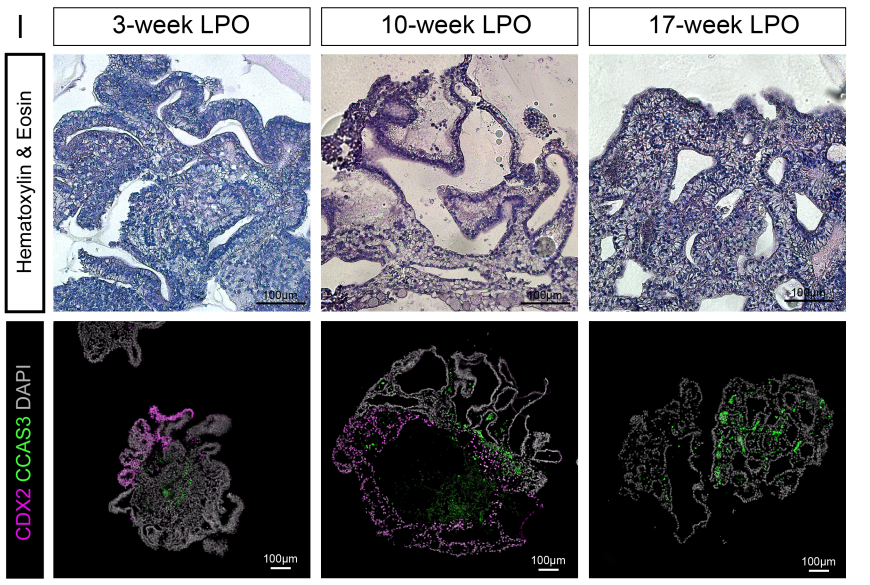

Fig. S2. Bud Tip Progenitors and Contaminating Lineages Emerge and Expand in LPOs Over Time, Related to Figure 2

(A) Maximum intensity projection of a whole mount immunofluorescence confocal Z-series staining of a 10-week LPO for bud tip progenitor markers CPM and SOX9 and lung epithelial marker NKX2-1.

(B) Maximum intensity projection of a whole mount immunofluorescence confocal Z-series staining of a 10-week LPO (left) or immunofluorescence staining on a paraffin section of 4-week LPOs (right) for intestinal epithelial marker CDX2 and lung epithelial marker NKX2-1.

(C) Representative flow cytometry plot for iBTP selection based on positive CPM and NKX2-1-EGFP selection on 10-week LPOs.

(D) (Left) FACS quantification of CPM^+ cells in LPOs in aggregate time course from three separate cell lines, including the NKX2-1-EGFP reporter line (iPSC17 WT 7B2), iPSC line 72.3 and WTC11. LPOs were sorted using CPM from 3 – 17 weeks in 3F media. Percentages of live cells expressing CPM (blue) or negative (grey) are reported as mean ± SEM for 3 – 9 replicates per time point. (Right) FACS quantification of CPM^+ cells in LPOs generated from spheroids using a previously published protocol (Miller *et al.*, 2019) from two separate cell lines, including the NKX2-1-EGFP reporter line and iPSC line 72.3 (WTC11-derived LPOs did not survive to 10 weeks) (Miller *et al.*, 2019).

(E) UMAP plot corresponding to the LPO cluster plot in Fig. 2G. Each dot represents a single cell and dots/cells are colored by the sample from which they came from.

(F) Stacked bar graph displaying the proportion of cells from each sample in each cluster of the LPO cluster plot in Fig. 2G.

(G) Dot plot of epithelial, mesenchymal, endothelial, and neuronal lineage genes as well as proliferation markers in each cluster of the LPO cluster plot in Fig. 2G. The dot size represents the percentage of cells expressing the gene in the corresponding cluster, and the dot color indicates log-normalized expression level of the gene.

(H) (Top) Stacked bar graph showing each cluster's normalized contribution to $KI67^+$ cells, calculated from the scRNA-seq data. (Bottom) Stacked bar graph showing each sample's normalized contribution to $KI67^+$ cells per cluster, calculated from the scRNA-seq data.

(I) (Top) Hematoxylin & eosin or (Bottom) immunofluorescence staining on paraffin sections of 3-, 10- and 17-week LPOs. IF stains for cell death marker cleaved caspase 3 (CCAS3) and intestinal epithelial marker CDX2.

Supplemental Figure 3

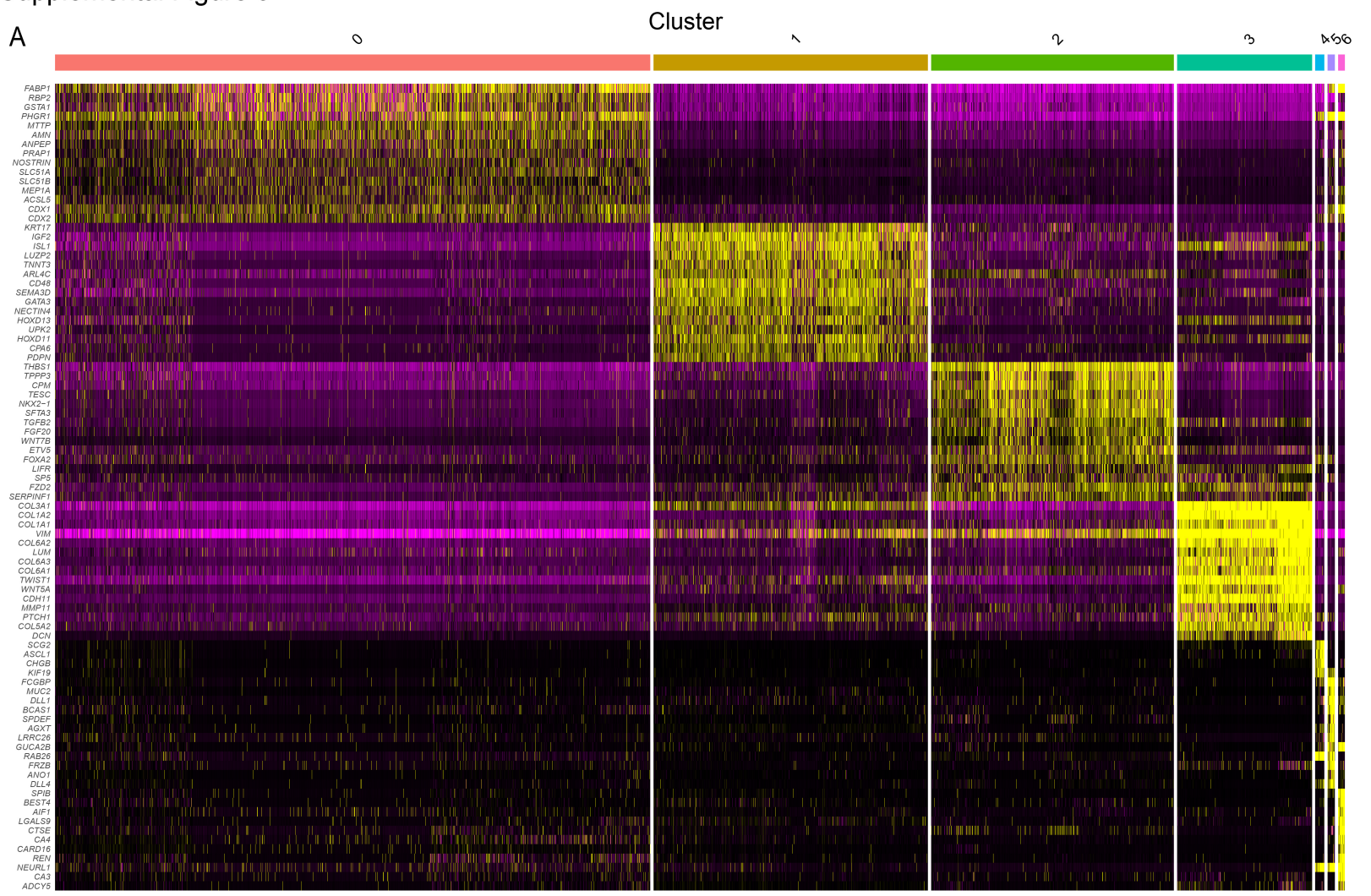

Fig. S3. LPOs are Transcriptionally Heterogenous

(A) Heat map including 12 genes per cluster picked from the top 50 highly enriched genes in each cluster corresponding to the UMAP cluster plot in Fig. 2G. Top-50 genes were based on log-fold change of each gene.

Supplemental Figure 4

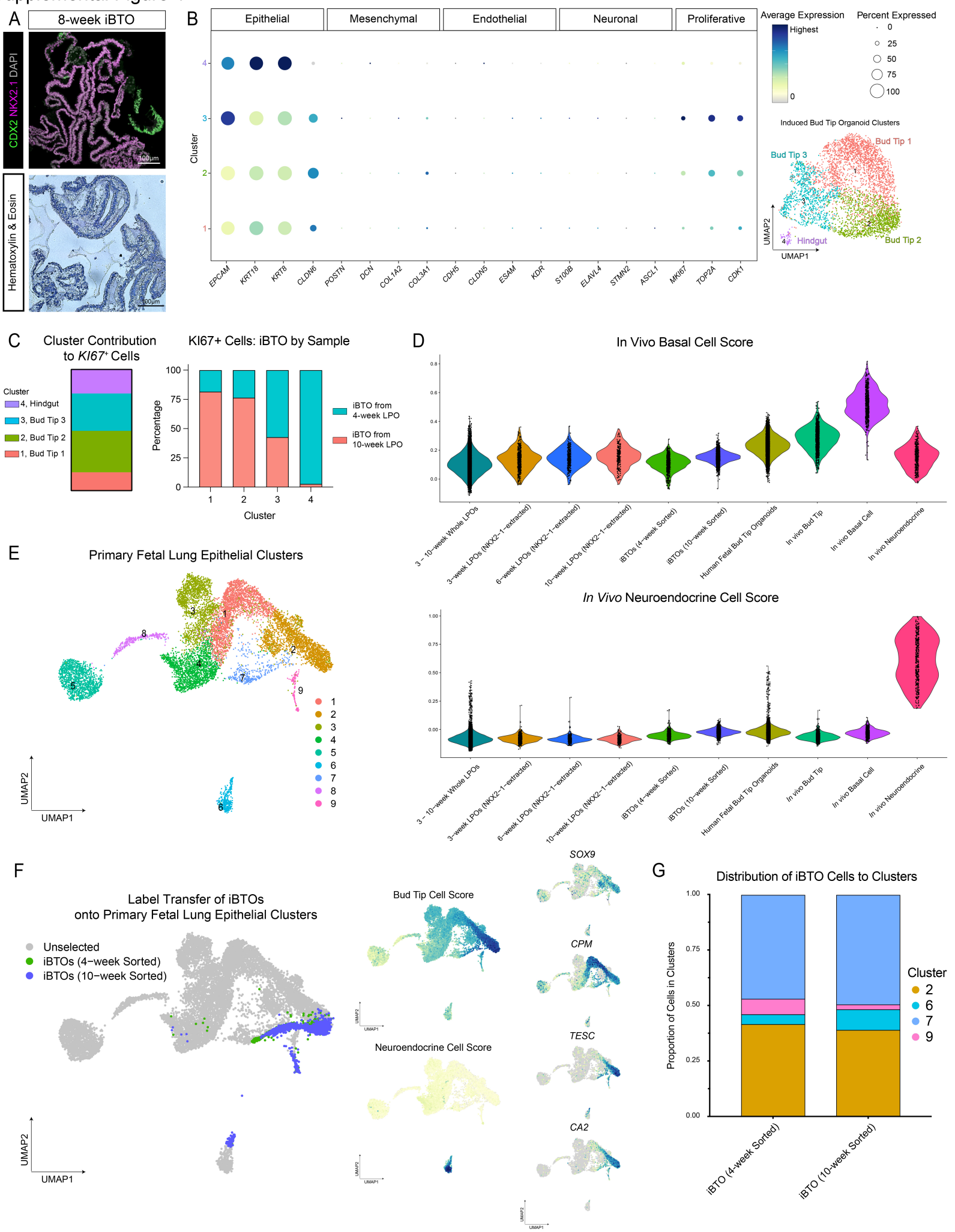

Fig. S4. Induced Bud Tip Organoids are Enriched for Bud Tip Progenitor Cells, Related to Figures 3 & 4

(A) (Top) Immunofluorescence staining on paraffin sections for lung epithelial marker NKX2-1 and intestinal epithelial marker CDX2 or (Bottom) hematoxylin & eosin stain on 8-week iBTOs.

(B) Dot plot of epithelial, mesenchymal, endothelial, and neuronal lineage genes as well as proliferation markers in each cluster of the iBTO cluster plot in Fig. 4A. The dot size represents the percentage of cells expressing the gene in the corresponding cluster, and the dot color indicates log-normalized expression level of the gene.

(C) (Left) Stacked bar graph showing each cluster's normalized contribution to $KI67^+$ cells, calculated from the scRNA-seq data. (Right) Stacked bar graph showing each sample's normalized contribution to $KI67^+$ cells per cluster, calculated from the scRNA-seq data.

(D) Violin plots displaying an *in vivo* basal (top) or neuroendocrine (bottom) cell score, calculated as the average expression of the top 100 enriched genes in *in vivo* basal or neuroendocrine cells, for each sample. Samples include whole LPOs (n = 2 for 3- and 6-week LPOs, n = 1 for 10-week LPOs), NXK2-1-extracted cells from 3-, 6-, and 10-week LPOs whole iBTOs (derived from LPOs sorted for $NKX2\text{-}1^+/CPM^+$ cells at 4 or 10 weeks, n=1 of each), human fetal-derived (primary) bud tip organoids, and primary *in vivo* tissue including computationally-extracted bud tip, basal, and neuroendocrine cells (Miller *et al.*, 2020; Hein *et al.*, 2022).

(E) UMAP cluster plot of previously-published scRNA-seq data from primary fetal lung epithelium spanning 8.5 – 21 weeks post-conception (n = 11 samples from trachea, airway, and distal bud tips) (Miller *et al.*, 2020; Hein *et al.*, 2022). Each dot represents a single cell and cells were computationally clustered based on transcriptional similarities. The plot is colored and numbered by cluster.

(F) Label transfer (Stuart *et al.*, 2019) of iBTO cells (derived from 4- or 10-week) sequenced via scRNA-seq onto the primary fetal lung epithelial UMAP embedding shown in Figure S4E. Feature plots display either an *in vivo* bud tip progenitor or *in vivo* neuroendocrine cell score, calculated as the average expression of the top 100 enriched genes in *in vivo* bud tip progenitor or neuroendocrine cells respectively, or single bud tip progenitor cell markers (*SOX9*, *CPM*, *TESC*, *CA2*). The color of each dot in the feature plot indicates log-normalized expression level of the individual genes or set of genes in the represented cell.

(G) Stacked bar graph displaying the percentage of iBTO cells from each timepoint that mapped to clusters 2, 6, 7, or 9 in the UMAP embedding shown in Figure S4E.

Supplemental Figure 5

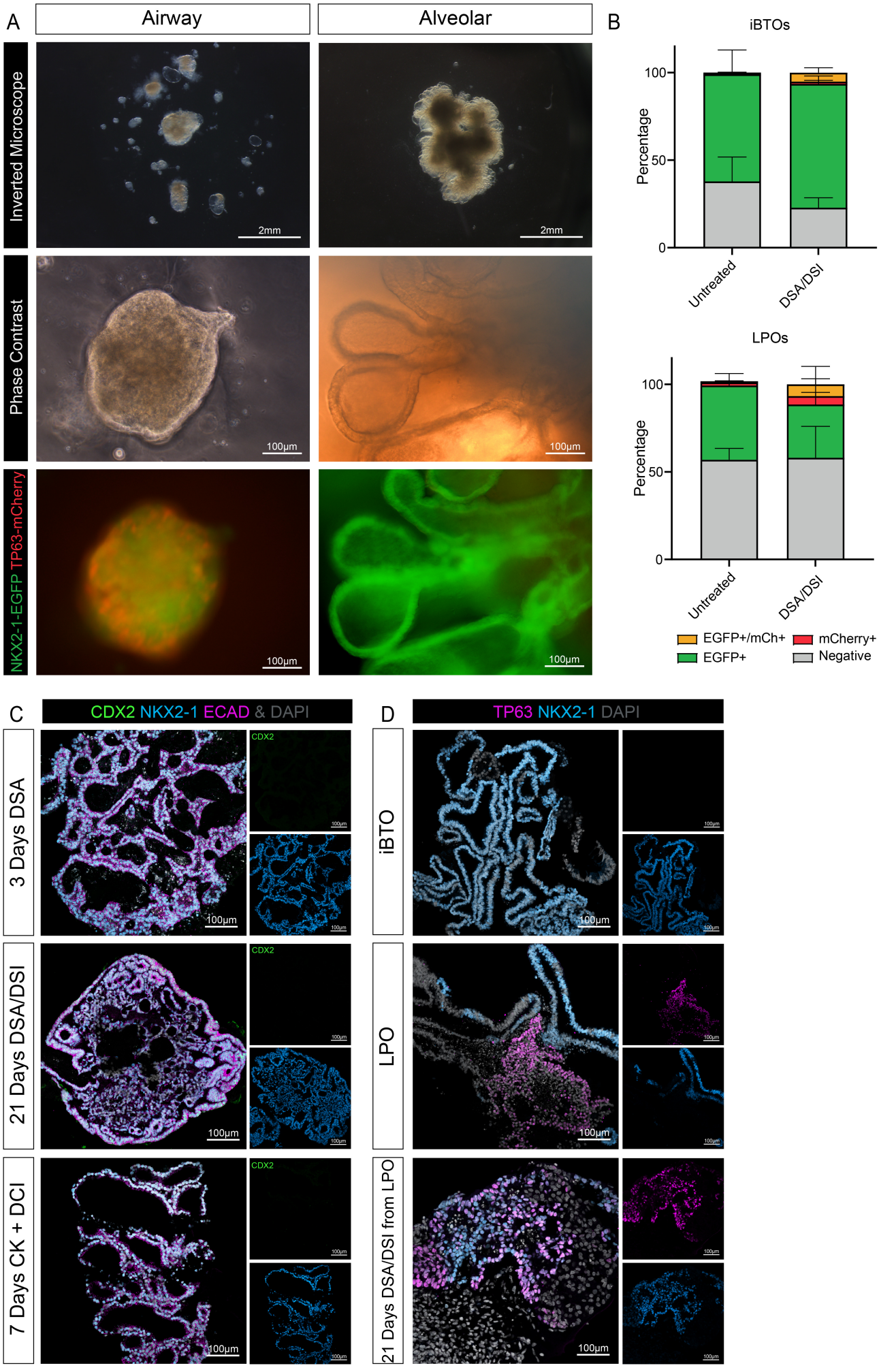

Fig. S5. iBTOs Maintain NKX2-1 Expression after Differentiation into Proximal Airway and Distal Alveolar Organoids, Related to Figure 5

(A) Representative brightfield, phase contrast, and reporter expression for NKX2-1-EGFP and TP63-mCherry images of iBTOs undergone the airway or alveolar induction protocol shown in Fig. 5A. Phase contrast and reporter images are from the same field of view.

(B) FACS quantification of NKX2-1-EGFP$^+$ and mCherry-TP63$^+$ cells from iBTOs and LPOs from the NKX2-1-EGFP/TP63-mCherry reporter cell line, (iPSC 17 WT 7B2) either in 3F media (untreated) or after 21 days of the airway differentiation protocol (DSA/DSI treatment). Percentages of live cells expressing neither reporter, each separate reporter, or dual-expressing are reported as mean ± SEM for 3 – 10 replicates per time point.

(C) Immunofluorescence staining on paraffin sections for the intestinal epithelial marker CDX2, lung epithelial marker NKX2-1, and general epithelial cell-type marker ECAD on 12-week iBTOs undergone the airway differentiation protocol (DSA/DSI treatment) or 3-week iBTOs undergone the alveolar differentiation protocol (7 days CK + DCI) (see Fig. 5A).

(D) Immunofluorescence staining on paraffin sections for the airway progenitor/basal cell marker TP63 and lung epithelial marker NKX2-1 on 12-week iBTOs, 4-week LPOs, and 3-week LPOs after 21 days of the airway differentiation protocol (DSA/DSI treatment).

Table S1. Cell Scoring Gene Lists

Click here to download Table S1

Table S2. Antibody and TSA Dilutions and Primer Sequences

Antibody	Dilution
FOXA2 (Seven Hills Bioreagents, Cat#WRAB-1200)	1:500
SOX17 (R&D Systems, Cat#AF1924)	1:500
VIM (R&D Systems, Cat#AFf2105)	1:500
TTF1/NKX2.1 (Abcam, Cat#ab76013)	1:500
SOX9 (Millipore, Cat#AB5535)	1:500
CPM (Wako/FujiFilm, Cat#014-27501)	1:500 for IF; 1:300 for FACS
CDX2 (BioGenex, Cat#MU392A-UC)	1:500
CDX2 (Cell Signaling Technology, Cat#12306) (Used only for co-stain with MUC2)	1:50
MUC2 (Santa Cruz Biotechnology, Cat#sc-515032)	1:300
Cleaved Caspase 3 (CCAS3) (Cell Signaling Technology, Cat#9664)	1:500
ECAD (R&D, Cat#AF748)	1:500
ECAD (BD Biosciences, Cat#610181)	1:500
SOX2 (R&D Systems, Cat#AF2018)	1:500
TP63 (R&D Systems, Cat#BAF1916)	1:500
CHGA (Santa Cruz Biotechnology, Cat#sc-1488)	1:100
FOXJ1 (Seven Hills Bioreagents, Cat#WMAB-319)	1:250
MUC5AC (Abcam, Cat#ab79082)	1:500

CC10/SCGB1A1 (Santa Cruz Biotechnology, Cat#sc-365992)	1:250
Acetylated Tubulin (AcTUB) (Sigma-Aldrich, Cat#T7451)	1:1000
ASCL1 (Santa Cruz Biotechnology, Cat#sc-374104)	1:50
Synaptophysin (SYN) (Abcam, Cat#ab32127)	1:500
SP-C (Santa Cruz Biotechnology, Cat#sc-518029)	1:200
Pro-SP-C (Seven Hills Bioreagents)	1:500
SP-B (Seven Hills Bioreagents, Cat#WMAB-1B9)	1:500
AffiniPure Donkey anti-Mouse IgG-AF488/Cy3/AF647 (Jackson ImmunoResearch, Cat#115-545-003, 115-165-003, 115-605-003)	1:500
AffiniPure Donkey anti-Goat IgG-AF488/Cy3/AF647 (Jackson ImmunoResearch, Cat#705-545-003, 705-165-003, 705-605-003)	1:500
AffiniPure Donkey anti-Rabbit IgG-AF488/Cy3/AF647 (Jackson ImmunoResearch, Cat#111-545-003, 111-165-003, 111-605-003)	1:500
Probe	**TSA dilution**
Hs-SCGB3A2-C2 (ACDbio RNAscope, Cat#549961-C2)	1:5000
Hs-SFTPB (ACDbio RNAscope, Cat#544251)	1:2500
Hs-MUC16-C2 (ACDbio RNAscope, Cat#40591-C2)	1:4000
Primer	**Sequence**
NKX2.1	F: CTCATGTTCATGCCGCTC R: GACACCATGAGGAACAGCG
CDX2	F: GGGCTCTCTGAGAGGCAGTT R: GGTGACGGTGGGGTTTAGCA

ECAD	F: TTGACGCCGAGAGCTACAC R: GACCGGTGCAATCTTCAAA
VIM	F: CTTCAGAGAGAGGAAGCCGA R: ATTCCACTTTGCGTTCAAGG
SOX2	F: GCTTAGCCTCGTCGATGAAC R: AACCCCAAGATGCACAACTC
TP63	F: CCACAGTACACGAACCTGGG R: CCGTTCTGAATCTGCTGGTCC
FOXJ1	F: CAACTTCTGCTACTTCCGCC R: CGAGGCACTTTGATGAAGC
CHGA	F: CTGTCCTGGCTCTTCTGCTC R: TGACCTCAACGATGCATTTC
MUC5AC	F: GCACCAACGACAGGAAGGATGAG R: CACGTTCCAGAGCCGGACAT
SCGB1A1	F: ATGAAACTCGCTGTCACCCT R: GTTTCGATGACACGCTGAAA
SCGB3A2	F: GGGGCTAAGGAAGTGTGTAAATG R: CACCAAGTGTGATAGCGCCTC
SFTPC	F: AGCAAAGAGGTCCTGATGGA R: CGATAAGAAGGCGTTTCAGG
SFTPB	F: GGGTGTGTGGGACCATGT R: CAGCACTTTAAAGGACGGTGT
ABCA3	F: TGCAGCGCCTACTTGAACTT R: CTGAGCACAGCCATCGTCT

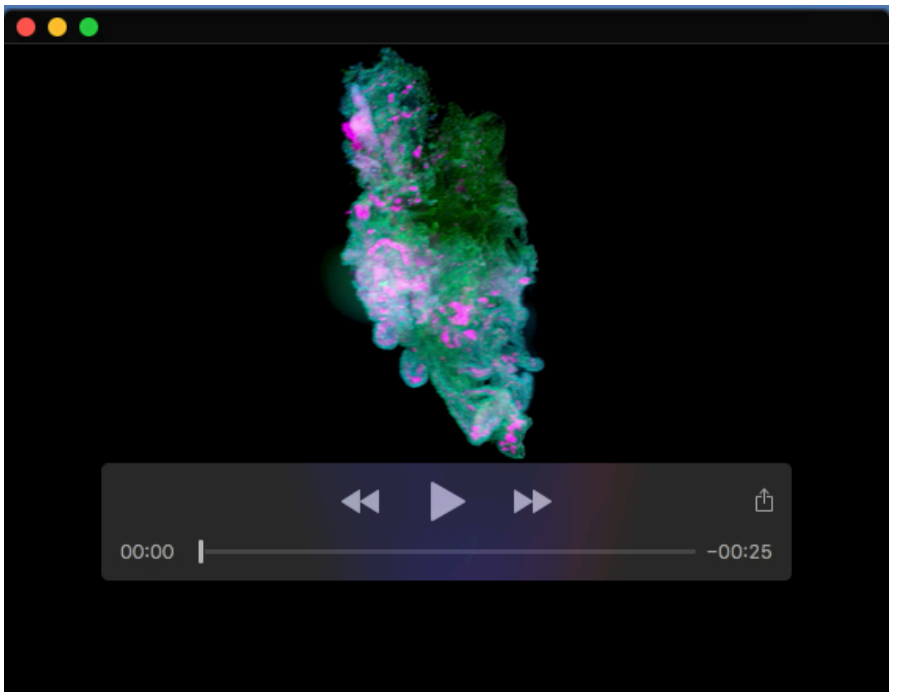

Movie 1. Bud Tip Progenitors in LPOs

Whole mount immunofluorescence confocal z-series staining of 10-week LPO for bud tip progenitor markers CPM (pink) and SOX9 (blue) and lung epithelial marker NKX2-1 (green).

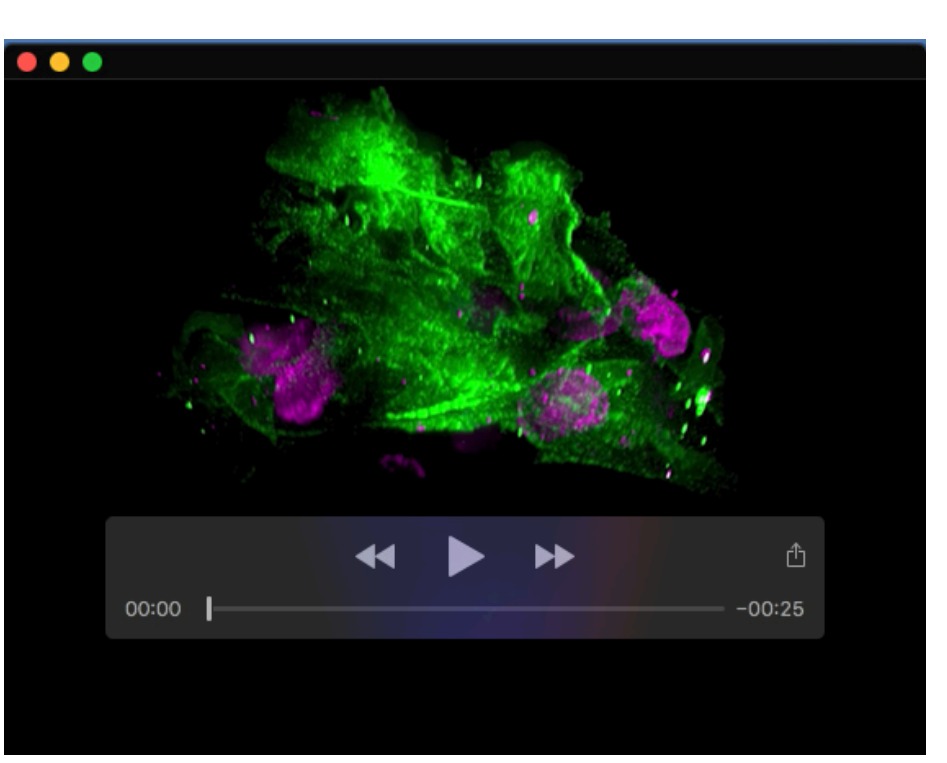

Movie 2. Lung and Intestine Regions in LPOs

Whole mount immunofluorescence confocal z-series staining of a 10-week LPO for lung epithelial marker NKX2-1 (green) and intestinal epithelial marker CDX2 (pink).

Supplementary Materials and Methods

Expression and Purification of Human Recombinant FGF10

The recombinant human FGF10 (rhFGF10) expression plasmid pET21d-FGF10 was a gift from James A. Bassuk (Bagai *et al.*, 2002) at the University of Washington School of Medicine. This plasmid was transformed to Novagen's Rosetta™ 2(DE3)pLysS competent cells (Millipore Sigma, Cat#71403-3) for rhFGF10 expression. In brief, *E.coli* strain Rosetta™ 2(DE3)pLysS bearing pET21d-FGF10 was grown in 2x YT medium (BD Biosciences, Cat#244020) with Carbenicillin (50 µg/mL) and Chloramphenicol (17 µg/mL). rhFGF10 expression was induced by addition of isopropyl-1-thio-β-D-galactopyranoside (IPTG). rhFGF10 was purified by using a HiTrap-Heparin HP column (GE Healthcare, Cat#17040601) with step gradients of 0.2 M to 0.92 M NaCl. From a 200 mL culture, 3 – 4 mg of at least 98% pure rhFGF-10 (evaluated by SDS-PAGE stained with Coomassie Blue R-250) was purified. In-house purified rhFGF10 was confirmed by western blot analysis using anti-FGF10 antibody and compared to commercially purchased rhFGF10 (R&D Systems, Cat#345-FG) to test/validate activity based on the efficiency to phosphorylate ERK1/2 in an A549 alveolar epithelial cell line (ATCC, Cat#CCL-185) as assessed by western blot analysis.

Expression and Purification of Human Recombinant FGF4

E.coli strain Rosetta™(DE3)pLysS bearing pET28/MhFGF4L was a gift from Masayuki Kobayashi (Sugawara *et al.*, 2014) at Akita Prefectural University, Japan. Culture of the *E.coli* strain was in 2X YT medium with Kanamycin (50 µg/mL) and Chloramphenicol (17 µg/mL). Expression and purification of rhFGF4 was performed as described above for rhFGF10. In-house purified rhFGF4 activity was compared to commercially purchased rhFGF4 (R&D Systems, Cat#235-F4) based on the efficiency to differentiate definitive endoderm cells from hPSCs into $CDX2^+$ hindgut cells by qRT-PCR and immunofluorescence (McCracken *et al.*, 2011).

Expression and Purification of Human Recombinant R-Spondin1

The stable 293T cell line expressing HA-R-Spondin1-Fc (Cultrex, Cat#3710-001-01) was cultured and passaged according to the manufacturer's protocol. For expression and purification, after at least five days in selection growth medium (0.3 mg/mL Zeocine), the cells were passaged to Triple Flasks (Nunc, Cat#132913) with 150-200 mL growth medium per flask without selection. The cells were cultured until they reached 90% confluency (~5 days), then medium was changed to CD293 medium (Gibco, Cat#11913-019) containing L-glutamine and Pen/Strep. Confluent cells were maintained in CD293 medium for 7 – 14 days, then the supernatant was collected and filtered for HA-R-Spondin1-Fc purification. The activity of the conditioned medium was determined by performing a TopFlash Luciferase Assay (Biotium, Cat#30085-2) by its ability to induce activation of Wnt/β-catenin. HA-R-Spondin1-Fc was purified using the Fc tag via protein A agarose purification kit (KPL, Cat#553-50-00) per manufacturer's instructions. From 1 L of conditioned medium, ~1.5 mg of at least 95% pure HA-R-Spondin1-Fc was purified. In-house purified HA-R-Spondin1-Fc activity was compared to commercially purchased rhR-Spondin1 (R&D Systems, Cat#4645-RS) based on the efficiency to differentiate $CDX2^+$ hindgut spheroids from hPSCs to human intestinal organoids (HIO) by qRT-PCR and HIO morphology (McCracken *et al.*, 2011).

SUPPLEMENTAL-SPECIFIC REFERENCES

Bagai, S. *et al.* (2002) 'Fibroblast growth factor-10 is a mitogen for urothelial cells', *The Journal of biological chemistry*. J Biol Chem, 277(26), pp. 23828–23837. doi: 10.1074/JBC.M201658200.

Sugawara, S. *et al.* (2014) 'Production of an aminoterminally truncated, stable type of bioactive mouse fibroblast growth factor 4 in Escherichia coli', *Journal of bioscience and bioengineering*. J Biosci Bioeng, 117(5), pp. 525–530. doi: 10.1016/J.JBIOSC.2013.10.009.